

# STUDY ON PHOTO-INDUCED DYNAMICS IN TOPOLOGICAL INSULATOR $\text{Bi}_2\text{Te}_3$ THIN FILMS

Kaishu Kawaguchi<sup>1</sup>, Ryo Mori<sup>1</sup>, Shinichiro Hatta<sup>2</sup>, Yuto Fukushima<sup>1</sup>, Hiroaki Tanaka<sup>1</sup>,  
Ayumi Harasawa<sup>1</sup>, Tetsuya Aruga<sup>2</sup>, Takeshi Kondo<sup>1</sup>

<sup>1</sup>*ISSP, The University of Tokyo*

<sup>2</sup>*Graduate School of Science, Kyoto University*

## INTRODUCTION

Spin-orbit interaction, where the orbital and spin components of electrons strongly intertwine, gives rise to distinctive electronic properties. Notably, due to their intimate relationship with topology, a variety of materials and functionalities in topological insulators have been actively researched in recent years. These materials, represented by  $\text{Bi}_2\text{Se}_3$ ,  $\text{Bi}_2\text{Te}_3$ , and others, have the interesting feature of having unique spin-polarized conduction electrons on their surfaces, even though their bulk is completely insulating [1]. Such novel materials have expected to be a highly promising foundation for the design of new electronic devices, such as quantum computing, spintronics, and so on. Angle-Resolved Photoemission Spectroscopy (ARPES) serves as a powerful experimental method to directly observe the electronic structure of these topological insulators, allowing us to analyze the behavior of electrons. Furthermore, with the incorporation of time-resolved techniques, ARPES opens the possibility to observe the dynamics of topological insulators in ultrafast time scales [2]. Time-resolved ARPES can observe how the electronic structure of materials changes by light pulses, thereby presenting a new way to control quantum properties.

In this study, we apply these advanced methods to thin films of topological insulators. By thinning these materials, interference effects can occur between surface and interface states, and potential modulation originating from the substrate becomes feasible. This will allow us to introduce novel perturbation effects to the properties of topological insulators from substrates. We anticipate that deepening our understanding of the dynamics and light-induced transitions in topological insulator thin films from a band picture will pave new horizons in opt-spintronics.

## METHODS

We carried out experiments using a thin film of the topological insulator  $\text{Bi}_2\text{Te}_3$ , fabricated on a *p*-type Si(111) substrate [3]. The research was measured by 10.7 eV pulse laser as a probe light source to the ARPES apparatus [4]. The optical energy of the pump pulse is set at 2.57 eV.

## RESULTS AND DISCUSSION

Figure 1 presents the results from time-resolved ARPES measurements of  $\text{Bi}_2\text{Te}_3$  thin films at 2 QL (quintuple layer). A photo-induced potential shift, namely surface photovoltage [5], were clearly observed. The maximum energy shift is approximately 0.3 eV, indicating a considerably large surface photovoltage in comparison with prior studies about single crystal of  $\text{Bi}_2\text{Te}_3$  [6]. The energy shift occurs on sub-nano seconds scale (Fig. 2), suggesting that this phenomenon originates from charge transfer near the surface or interface;  $\text{Bi}_2\text{Te}_3$  thin film is unlikely to induce sufficient charge transfer within thickness of 2 nm in this case, therefore the 0.3 eV energy shift is likely to be due to photoexcitation of band bends originating from the *p*-type Si(111) substrate as the mechanism. Based on these results, utilizing a highly doped substrate can be considered an effective method to induce a photoelectric field in thin films. In the future, the doping dependence of the substrate and the thickness dependence of the thin film will be studied to investigate the possibility of controlling the electronic state by surface photovoltages.

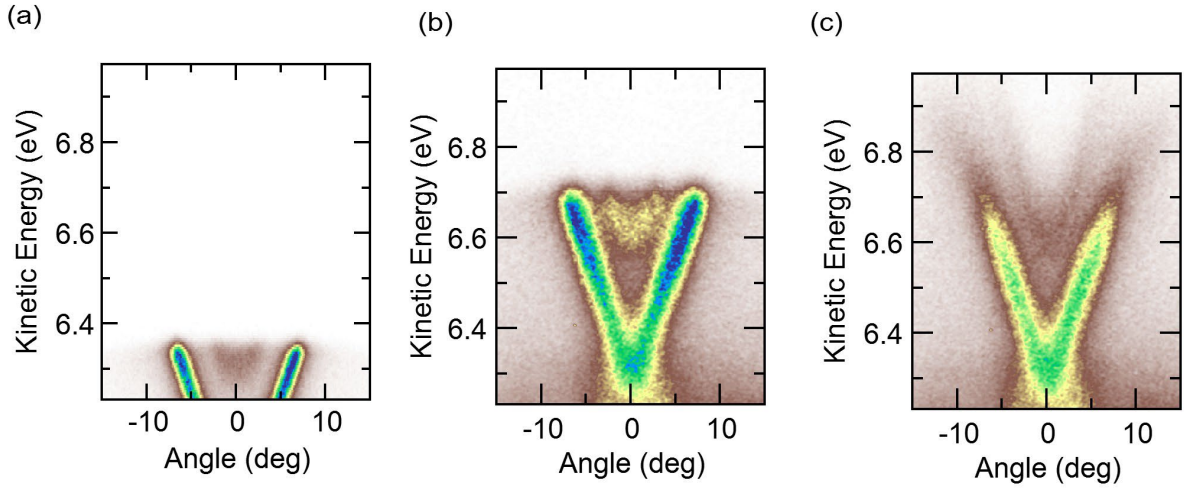


Fig. 1 : Time-resolved ARPES results of  $\text{Bi}_2\text{Te}_3$  thin film at 2 QL thickness. (a) is the ground state without the pump pulse. (b) and (c) are the results at delay times of -1 ps (before arriving the pump pulse) and 0 ps (after arriving the pump pulse), respectively.

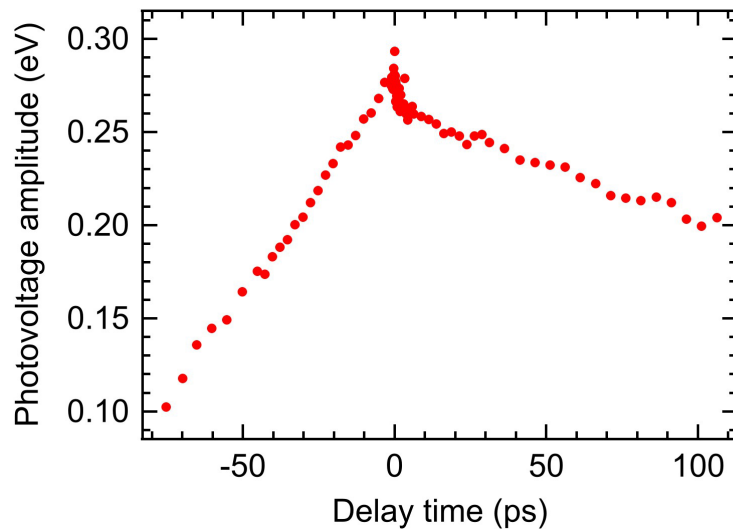


Fig. 2 : Time evolution of surface photovoltage amplitude estimated from the peak position of the band dispersion, where delay time is the time difference between the pump and probe pulse.

## REFERENCES

- [1] H. Zhang *et al.*, Nat. Phys. **5**, 438 (2009).
- [2] J. A. Sobota *et al.*, Phys. Rev. Lett. **108**, 117403 (2012).
- [3] S. Hatta *et al.*, Sci. Rep. **11**, 5742 (2021).
- [4] K. Kawaguchi *et al.*, arXiv:2303.16466 (2023).
- [5] D. K. Schroder, Meas. Sci. Technol. **12**, R16 (2001).
- [6] S. Ciocys *et al.*, npj Quantum Materials. **5**, 1–7 (2020).

# FERMI SURFACE MAPPING OF TOPOLOGICAL INSULATOR $\text{Pb}(\text{Bi}_{0.3}\text{Sb}_{0.7})_2\text{Te}_4$

Koichiro YAJI<sup>1</sup>, Yuya HATTORI<sup>2</sup>, Shunsuke YOSHIKAWA<sup>1</sup>, Shunsuke TSUDA<sup>1</sup>,  
Youhei YAMAJI<sup>3</sup>, Yuto FUKUSHIMA<sup>4</sup>, Kaishu KAWAGUCHI<sup>4</sup>, Takeshi KONDO<sup>4</sup>,  
Yuki TOKUMOTO<sup>5</sup>, Keiichi EDAGAWA<sup>5</sup>, and Taichi TERASHIMA<sup>2</sup>

<sup>1</sup>*Research Center for Advanced Measurement and Characterization, NIMS*

<sup>2</sup>*International Center for Materials Nanoarchitectonics, NIMS*

<sup>3</sup>*Center for Green Research on Energy and Environmental Materials, NIMS*

<sup>4</sup>*Institute for Solid State Physics, The University of Tokyo*

<sup>5</sup>*Institute of Industrial Science, The University of Tokyo*

Topological materials are placed at a central research field in solid-state physics and materials science. Topological surface states (TSSs) are formed through a phase transition from a trivial insulator to a topological insulator, the so-called topological phase transition. The topological phase transition has been experimentally demonstrated in several systems, where the bulk band inversion is artificially controlled by changing the composition and modulating the lattice constant, etc. In contrast, experimental studies on the topological phase transition in pristine topological materials have not been established so far, even though examining it helps us understand the fundamental electronic properties of the topological materials. In the present study, we have performed the Fermi surface mapping of  $\text{Pb}(\text{Bi}_{0.3}\text{Sb}_{0.7})_2\text{Te}_4$  to elucidate the electronic band structure. Here, the Pb-based ternary compounds,  $\text{Pb}(\text{Bi}_{1-x}\text{Sb}_x)_2\text{Te}_4$ , is known as a strong topological insulator, which have been confirmed by angle-resolved photoemission spectroscopy [1–3]. This work is part of a project to elucidate topological phase transitions in pristine materials.

Laser-ARPES measurements have been performed at the Institute for Solid State Physics, The University of Tokyo [4]. The samples were cleaved with scotch tape in an ultra-high vacuum chamber. The photoelectrons were excited by lasers with photon energies of 6.994 eV [5] and 10.7 eV [6]. We used a p-polarized light. The sample temperature was kept at 30 K during the measurements.

Figures 1(a) and (b) show the ARPES intensity map along  $\Gamma\text{M}$  and constant energy contours of. Figure 1(b) shows constant energy contours  $\text{Pb}(\text{Bi}_{0.3}\text{Sb}_{0.7})_2\text{Te}_4$  with an excitation energy ( $h\nu$ ) of 6.994 eV. Above the Dirac point (DP), the constant energy contours gradually change from circular to hexagonal shapes: the constant energy contour at  $E_B = 110$  meV is circular, at  $E_B = 70$  meV hexagonal, and at  $E_B = 30$  meV the conduction band appears at  $\Gamma$ . In contrast, a strong warping effect appear in the constant energy contours below the DP. The constant energy contours at  $E_B = 330$  meV is elongated in  $\Gamma\text{M}$ .

Photoexcitation with a 10.7 eV laser allows us to investigate a wider wavenumber range [Fig. 1(c)]. The photoelectron intensity distribution of the constant energy contours with  $h\nu = 10.7$  eV is different from  $h\nu = 6.994$  eV, resulting from the final state effect in photoemission. In the contours at  $E_B = 190$  meV, corresponding to the DP, and  $E_B = 260$  meV, a sole surface state (or surface resonance) is observed around  $\Gamma$  in each image, meaning that the valence band maximum (VBM) for  $x = 0.70$  is located at  $\Gamma$ . At  $E_B = 330$  meV, a steeply elongated surface resonance is observed in  $\Gamma$ . Therefore, the energy dispersions of the surface resonances are moderate along  $\Gamma$  while they are steep away from  $\Gamma\text{M}$ .

The previous theoretical calculations suggest that the VBM for  $x = 0.0$  is located at  $k = \pm 0.3 \text{ \AA}^{-1}$  in  $\Gamma$  with the energy position comparable to the DP, while the VBM for  $\text{PbSb}_2\text{Te}_4$  (i.e.  $x =$

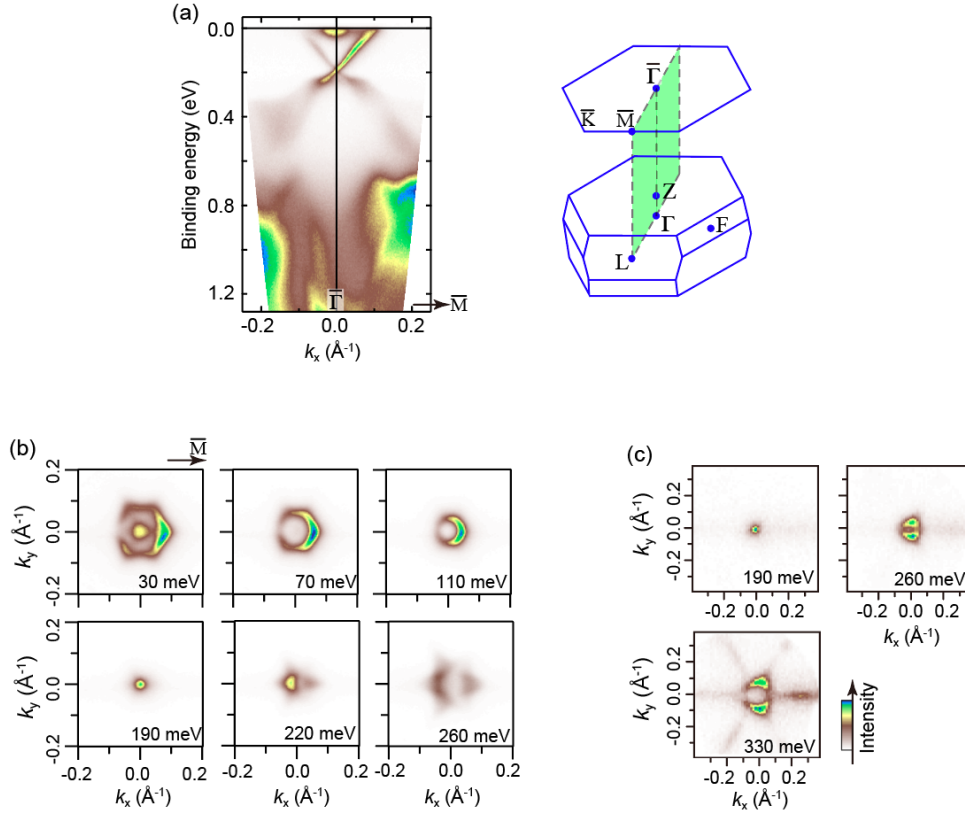


Fig. 1 (a) ARPES intensity images recorded along  $\Gamma\bar{M}$  for  $\text{Pb}(\text{Bi}_{0.3}\text{Sb}_{0.7})_2\text{Te}_4$ . [7] (B,C) Constant energy contours of the ARPES intensity taken with  $h\nu = 6.994$  eV [7] and 10.7 eV photons, respectively.

1.0) is located at  $\Gamma$  with the energy 200 meV lower than the DP [1]. In the previous ARPES study for  $x = 0.0$ , the band at  $k = \pm 0.3 \text{ \AA}^{-1}$  in  $\Gamma$  is located at 20 meV lower energy than the DP, which is assigned as the VBM [3]. The present study reveals that in the case of  $x = 0.70$ , the band at  $k = \pm 0.3 \text{ \AA}^{-1}$  in  $\Gamma$  is found in a deeper binding energy side by 100 meV than the energy of the DP. Our ARPES suggests that the band energy at  $k = 0.3 \text{ \AA}^{-1}$  in  $\Gamma$  can be tunable by the replacement of Bi with Sb.

## REFERENCES

- [1] T. V. Menshchikova, S. V. Eremeev, E. V. Chulkov, *Applied Surface Science* **267**, 1 (2013).
- [2] S. Souma, K. Eto, M. Nomura, K. Nakayama, T. Sato, T. Takahashi, K. Segawa, and Y. Ando, *Phys. Rev. Lett.* **108**, 116801 (2012).
- [3] K. Kuroda, H. Miyahara, M. Ye, S. V. Eremeev, Y. M. Koroteev, E. E. Krasovskii, E. V. Chulkov, S. Hiramoto, C. Moriyoshi, Y. Kuroiwa, K. Miyamoto, T. Okuda, M. Arita, K. Shimada, H. Namatame, M. Taniguchi, Y. Ueda, and A. Kimura, *Phys. Rev. Lett.* **108**, 206803 (2012).
- [4] K. Yaji, A. Harasawa, K. Kuroda, S. Toyohisa, M. Nakayama, Y. Ishida, A. Fukushima, S. Watababe, C.-T. Chen, F. Komori, and S. Shin, *Rev. Sci. Instrum.* **87**, 053111 (2016).
- [5] T. Shimojima, K. Okazaki, and S. Shin, *J. Phys. Soc. Jpn.* **84**, 072001 (2015).
- [6] K. Kawaguchi, K. Kuroda, Z. Zhao, S. Tani, A. Harasawa, Y. Fukushima, H. Tanaka, R. Noguchi, T. Iimori, K. Yaji, M. Fujisawa, S. Shin, F. Komori, Y. Kobayashi, and Takeshi Kondo, *submitted*.
- [7] K. Yaji, Y. Hattori, S. Yoshizawa, S. Tsuda, F. Komori, Y. Yamaji, Y. Fukushima, K. Kawaguchi, T. Kondo, Y. Tokumoto, K. Edagawa, T. Terashima, *submitted*.

# DIRECT OBSERVATION OF QUANTUM WELL STATES INDUCED BY THE HYDROGEN-BONDED ORGANIC FRAMEWORKS FORMED ON METAL SURFACE

Kaname Kanai<sup>1</sup>, Rena Moue<sup>1</sup>, Hiroto Yamazaki<sup>1</sup>, Kaishu Kawaguchi<sup>2</sup>, Ryo Mori<sup>2</sup>, Yuto Fukushima<sup>2</sup>, Ayumi Harasawa<sup>2</sup>, Shik Shin<sup>2</sup>, Takeshi Kondo<sup>2</sup>

*Faculty of Science and Technology Tokyo University of Science<sup>1</sup>, The Institute for Solid State Physics, The University of Tokyo<sup>2</sup>*

The capability to control the electronic properties of the material surface is essential for the development and optimization of applications involving interfacial electron transfer, such as optoelectronic devices and photovoltaic devices. Therefore, noble metal (111) surfaces are of particular interest due to their unique susceptibility to the presence of adsorbates due to their electronic structure. In fact, the two-dimensional free electron-like Shockley state (SS) localized at the  $\Gamma$  point of the noble metal (111) surfaces is easily modulated by periodic potentials formed by regularly adsorbed atoms and molecules<sup>[1-3]</sup>. This change in SS at the noble metal surface can be revealed by observing the change in its energy band dispersion. For example, it is known to appear as a change in Rashba effect. The effect is an effect in which spin-orbit interactions due to spatial inversion symmetry breaking at the noble metal surface causes spin splitting in the SS. The magnitude of the effect is highly dependent on its surface states. It is also known that the formation of a molecular layer with corrals on the noble metal can form quantum confinement by confining SS, that is, the surface free electrons, in the corrals. Recently, in order to investigate the latter, the focus has been on observing the effects of self-organized ordered layers with large corrals on the surface electronic structure<sup>[3, 4]</sup>. This is potentially problematic because the properties of the electronic states are inherently sensitive to defects in the self-assembled molecular layer. Another approach to compensate for the imperfections in self-assembly is to use a ring of molecules such that each individual molecule acts as a corral to confine electrons. This allows each molecule to form nearly identical confinement potential, forming a long-range defect-free quantum confined surface states (QCSS)<sup>[5]</sup>.

In this study, we investigated the effect of a self-assembled film of [8]cycloparaphenylene ([8]CPP) (figure 1a), which has a ring-shaped molecular structure, on the SS of Au(111). The adsorption structure of [8]CPP was determined by low-energy electron diffraction (LEED) and the energy band dispersion was directly observed by angle-resolved photoemission spectroscopy (ARPES).

Figure 1b shows the experimental (exp.) and calculation (cal.) results of LEED with stepwise increasing coverage of [8]CPP monolayers on Au(111). Furthermore, the adsorption structures of [8]CPP with different coverage were determined from the LEED results. From left to right, the results correspond to about 3, 5, and

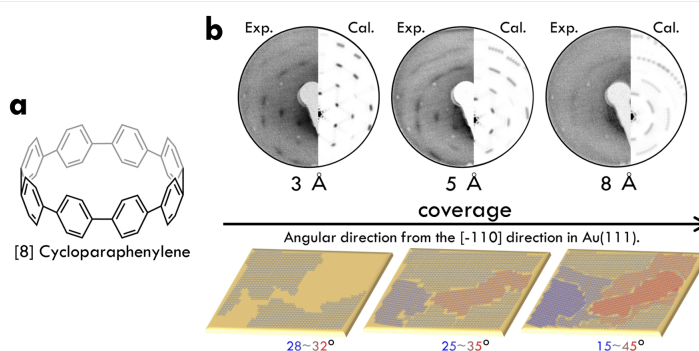


Figure 1. a) Molecular structures of [8]CPP. b) Experimental and simulated LEED results for [8]CPP/Au(111) and schematic of the [8]CPP growth process on Au(111). The right half of the circle shows the LEED pattern observed at the primary energy of  $E_p=25$  eV (exp.). The left half of the circle shows the LEED pattern simulated by calculation (cal.). The bottom row of b) shows a schematic of the growth process of the [8]CPP monolayer on Au(111) obtained from the LEED results shown in the top row. When [8]CPP coverage is 3, 5, and 8 Å, the adsorption structure is formed along the angular direction of 28~32°, 25~35° and 15~45° from the [-110] direction in Au(111).

8 Å coverage of [8]CPP, respectively, and it was confirmed that [8]CPP forms an adsorption structure as if flatly adsorbed on the Au(111) surface, a result similar to previous studies<sup>[5]</sup>. In addition, we confirmed that the growth direction of the adsorption structure diffused as the coverage increased. In short, this study revealed for the first time that the adsorbed structures gradually become multi-domain as the coverage increases.

The changes in SS observed by ARPES in accordance with the changes in the adsorption structure of the revealed [8]CPP are shown in figure 2. Figures 2a, c, e, and g are band mappings by ARPES, and figures 2b, d, f, and h are second-order derivative (SOD) results to clarify the features. Figures 2a and b show the SS of Au(111), where the spin splitting (Rashba splitting) due to the Rashba effect is clearly visible. In [8]CPP(3 Å)/Au(111), where few multi-domains are observed, the bottom of the energy band dispersion representing the SS is flattened (figures 2c, d). In [8]CPP(5 Å)/Au(111), where the multi-domains were clearly observed, the flattened energy band dispersion (flat band) was obscured, but the Rashba splitting was again confirmed with a shift of about 0.1 eV to the low binding side (figures 2e, f). In addition, the Brillouin zone was modulated by the super-periodic structure formed by [8]CPP, and a new energy band dispersion was also observed due to the folding of the Au(111) *sp* band. In [8]CPP(8 Å)/Au(111), where multi-domains dominate, the flat band disappear and the energy band dispersion indicative of Rashba splitting and folding are obscured (figures 2g, h). The analysis revealed that the magnitude of Rashba splitting is about 18% when [8]CPP was adsorbed at about 5 Å. The flat band observed at 3 and 5 Å adsorption suggest quantum confinement caused by the confinement of surface electrons in the corral. However, the flat band are weakly dispersive because the confinement by organic molecules is incomplete and the electrons trapped in the corrals interact with each other to form a dispersion.

In this study, we observed the formation of [8]CPP on Au(111). As a result, we revealed for the first time the formation of multi-domains with increasing coverage. In addition, the surface electronic states in each were observed by ARPES, which affected the Rashba effect on the Au(111) surface and suggested the formation of quantum confinement.

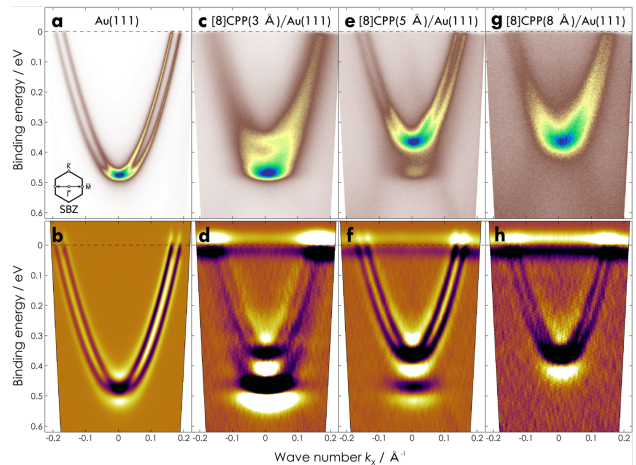


Figure 2. Band mapping around the  $\Gamma$  point of a) clean Au(111) by ARPES. The lower left corner of the figure shows the measured orientation in the  $k$ -space in the schematic of the surface Brillouin zone (SBZ). b) SOD of the band mapping by ARPES of clean Au(111) versus energy. The black areas on the SOD represent the electronic states. Band mapping around the  $\Gamma$  point of c) [8]CPP(3 Å)/Au(111), d) [8]CPP(5 Å)/Au(111) and e) [8]CPP(8 Å)/Au(111) by ARPES. Band mapping based on the SODs of the corresponding ARPES results, f) d), g) f), h).

## REFERENCES

- [1] C. R. Ast *et al.*, *Phys. Rev. Lett.*, **98**, 186807 (2007).
- [2] J. Zroff *et al.*, *Surface Science*, **603**, 354-358 (2009).
- [3] I. Piquero-Zulaica *et al.*, *Nat. Commun.*, **8**, 787 (2017).
- [4] J. Zhang *et al.*, *Chem. Commun.*, **50**, 12289-12292 (2014).
- [5] B. N. Taber *et al.*, *J. Phys. Chem. Lett.* **7**, 3073-3077 (2016).

# SPIN- AND ANGLE-RESOLVED PHOTOEMISSION STUDY OF MAX PHASE COMPOUND ZR<sub>3</sub>SNC<sub>2</sub>

Takahiro Ito<sup>1,2</sup>, Manaya Mita<sup>2</sup>, Kiyohisa Tanaka<sup>3</sup>, Masashi Nakatake<sup>4</sup>, Yuto Fukushima<sup>5</sup>, Kaishu Kawaguchi<sup>5</sup>, Takeshi Kondo<sup>5</sup>, Laurent Jouffret<sup>6</sup>, Hanna Pazniak<sup>7</sup>, Serge Quessada<sup>7</sup> and Thierry Ouisse<sup>7</sup>

<sup>1</sup>Synchrotron radiation Research center (NUSR), Nagoya University, Nagoya 464-8603, Japan

<sup>2</sup>Graduate School of Engineering, Nagoya University, Furo-cho, Chikusa, Nagoya 464-8603, Japan

<sup>3</sup>Institute for Molecular Science, Okazaki 444-8585, Japan

<sup>4</sup>Aichi Synchrotron Radiation Center, Seto, 489-0965, Japan

<sup>5</sup>Institute for Solid State Physics, Th University of Tokyo, Kashiwa 277-8581, Japan

<sup>6</sup>Université Clermont Auvergne, CNRS, ICCF, F-63000 Clermont–Ferrand, France

<sup>7</sup>Univ. Grenoble Alpes, CNRS, Grenoble INP, LMGP, F-38000 Grenoble, France

MAX phases ( $M_{n+1}AX_n$ , where M is an early transition metal, A belongs to groups 13-15 and X is either C or N,  $n = 1 - 3$ ) have recently attracted much attention due to their possible application to the production of a new class of two-dimensional (2D) systems called MXenes [1]. However, the bulk electronic structure of MAX phases has been studied mostly through *ab initio*, DFT calculations, mainly due to a lack of single crystalline samples. We have performed angle-resolved photoemission spectroscopy (ARPES) on several MAX phase single crystals to directly investigate the electronic structure of these systems [2-5]. Among the MAX phases, Zr<sub>3</sub>SnC<sub>2</sub> is characterized by relatively higher two-dimensionality than 211 phase due to the thicker MX layer. In addition, the strong spin-orbit coupling effect due to the 4d transition metal Zr is expected. We have performed SARPES study on Zr<sub>3</sub>SnC<sub>2</sub> to elucidate the electronic and spin structures with using He I light source, which is available for the spin mapping at the wide momentum space.

Figures 1(a(b)) and (c) show the band structure (which compared with DFT calculation along  $\Gamma M$  line of the Sn-terminated surface) and the constant energy ARPES image at 3.1 eV

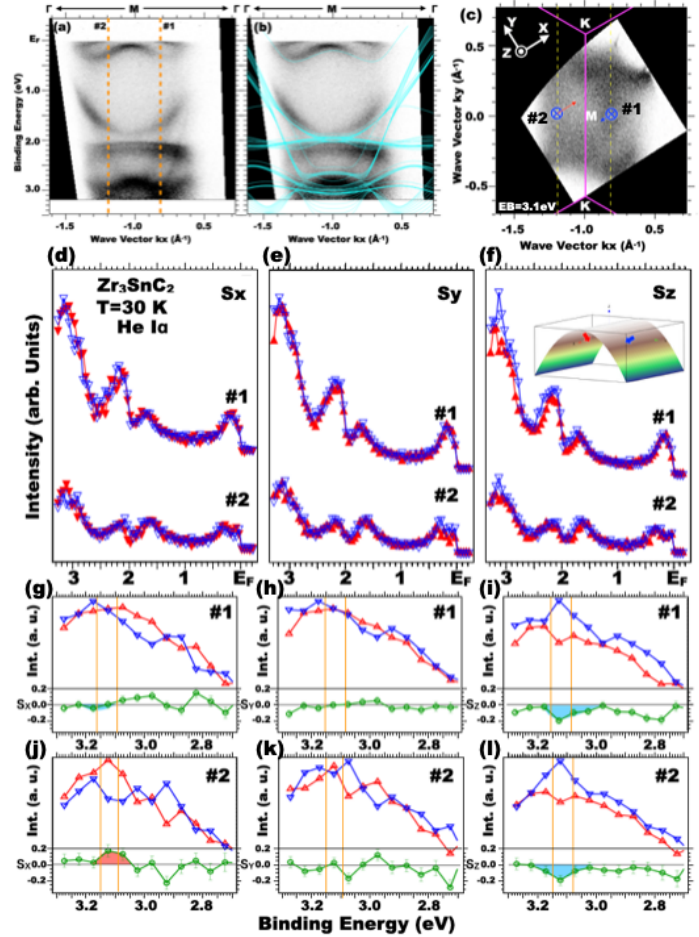


**Fig. 1:** (a) Band structure along the  $\Gamma M$  line of Zr<sub>3</sub>SnC<sub>2</sub>. (b) Same as (a) but compared with DFT calculation (light blue lines) of the Sn-terminated surface. (c) Constant energy ARPES image at 3.1 eV around the M point. The definition of the spin polarization directions ( $S_x$ ,  $S_y$  and  $S_z$ ) projected on the sample surface are indicated by white arrows, respectively. (d-f) SARPES spectra ( $S^+$ :  $\blacktriangle$ ;  $S^-$ :  $\nabla$ ) at momentum cut#1 and #2 in Figs. 1(a) and (c) of  $S_x$  (a),  $S_y$  (b) and  $S_z$  (c), respectively. (g-l) Enlarged SARPES spectra around 3.1 eV. Spin polarization is shown at the bottom of each panel.

eV, respectively. From the comparison with DFT calculation, it has been found that the electronic structure of  $Zr_3SnC_2$  around the M point has been well reproduced by the Sn-terminated surface states, typically saddle-like dispersive feature just below the Fermi level.

While there is no clear sign of spin-polarization at the low binding energy side, we found that non-negligible spin-polarization seems to be observed around 3.1 eV. In Fig. 1(i) and (l), out-of-plane spin polarization ( $S_z$ ) shows sizable  $S_z^-$  sign at both cut#1 and #2. On the other hand, in-plane spin polarization  $S_x$  shows  $S_x^+$  sign at cut#2 (Fig. 1(j)). Furthermore, there is no clear sign of in-plane spin polarization along y (Fig. 1(h) and (k)). From the observed spin textures, we expect the possible existence of out-of-plane spin polarization at “bridge-like” band dispersion around 3.1 eV as shown in the inset of Fig. 1(f), though the symmetrically required antiparallel  $S_x^-$  component has not been clearly observed. These results might suggest the effect of Dresselhaus spin-orbit coupling causing the out-of-plane spin texture [6] at the Sn-terminated surface of  $Zr_3SnC_2$ . To clarify the mechanisms of the formation of the observed spin-states and prove their existence, further ARPES study choosing surface termination as well as DFT calculation of spin-texture will be performed in our future work.

## REFERENCES

- [1] M. Barsoum, MAX phases (Wiley, Weinheim 2013).
- [2] T. Ito *et al.*, Phys. Rev. B **96**, 195168 (2017).
- [3] D. Pinek *et al.*, Phys. Rev. B **98**, 035120 (2018).
- [4] D. Pinek *et al.*, Phys. Rev. B **102**, 075111 (2020).
- [5] D. Pinek *et al.*, Phys. Rev. B **104**, 195118 (2021).
- [6] L. L. Tao *et al.*, Nature Commun. **9**, 2767 (2018).



# HIGH-RESOLUTION TEMPERATURE DEPENDENT SPIN-RESOLVED PHOTOEMISSION SPECTROSCOPY OF HALF-METALLIC FERROMAGNET $\text{La}_{1-x}\text{Sr}_x\text{MnO}_3$

Takayoshi YOKOYA<sup>1</sup>, Noriyuki KATAOKA<sup>1</sup>, Takanori WAKITA<sup>1</sup>, Hirokazu FUJIWARA<sup>2</sup>, Yuto FUKUSHIMA<sup>2</sup>, Kaishu KAWAGUCHI<sup>2</sup>, Hiroaki TANAKA, Ryo MORI<sup>2</sup>, Ayumi HARASAWA<sup>2</sup>, Takeshi KONDO<sup>2</sup>, Hiroshi KUMIGASHIRA<sup>2</sup>, Yuji MURAOKA<sup>3</sup>

<sup>1</sup>*Research Institute for Interdisciplinary Science, Okayama University*

<sup>2</sup>*Institute for Solid State Physics, The University of Tokyo*

<sup>3</sup>*Institute of Multidisciplinary Research for Advanced Materials, Tohoku University*

Half metallic ferromagnets have a unique spin dependent electronic structure near the Fermi level ( $E_F$ ), where only one of the spin states crosses  $E_F$  and the other has an energy gap across  $E_F$  [1]. The unique electronic structure gives rise to many-body effects different from other systems. Theoretically, the electronic states induced by many-body effects in half metals has been proposed as non quasiparticle (NQP) states [2]. The experimental verification for NQP states was made recently for a half metallic ferromagnet  $\text{CrO}_2$  by using high-resolution (HR) spin-resolved photoemission spectroscopy (SRPES) [3]. In the present research, we have performed HRSRPES of another half metallic ferromagnet  $\text{La}_{1-x}\text{Sr}_x\text{MnO}_3$  to experimentally explore the characteristics and universality of NQP states.  $\text{La}_{1-x}\text{Sr}_x\text{MnO}_3$  is one of the famous perovskite materials, exhibiting colossal magnet resistance around Sr concentration  $x$  of 0.3.

Homoepitaxial films of  $\text{La}_{1-x}\text{Sr}_x\text{MnO}_3$  were grown on the atomically-flat (001) surface of Nb-doped  $\text{SrTiO}_3$  substrates using a laser MBE method. Laser-based HRSRPES experiments were performed at the Institute for Solid State Physics, The University of Tokyo [4]. The  $p$ -polarized light with  $h\nu = 6.994$  eV was used to excite the photoelectrons. Photoelectrons were analyzed with a combination of a ScientaOmicron DA30L analyzer and a very-low-energy-electron-diffraction (VLEED) type spin detector. During the measurement, the instrumental energy resolution was set to 30 meV to compensate small electron counts and the base pressure was kept below  $1 \times 10^{-8}$  Pa. Calibration of the Fermi edge ( $E_F$ ) for the samples was achieved using a gold reference. The data were taken at  $T = 20, 50, 90, 110, 135, 195$  and 300 K. The sample was annealed at 400 K under oxygen atmosphere prior to the experiment. We magnetized the  $\text{La}_{1-x}\text{Sr}_x\text{MnO}_3(001)$  sample along the magnetic easy axis ([110] direction) by bringing the sample close to a magnet. The approximate magnitude of the magnetic field at the sample position was 700 Oe.

Figure 1 shows the temperature dependent HRSRPES data. At 20 K, the spectrum of the majority spin states shows a Fermi edge, while that of the minority spin states shows negligible intensity near  $E_F$ . Accordingly, the polarization is nearly 100% near  $E_F$ , providing spectroscopic evidence for half metallicity of the sample at 20 K. In increasing temperature, the spectra of the majority and minority spin states, as well as the polarization, do not show drastic changes till

195 K. At 300 K, the spectral shapes of the majority and minority spin states become similar and the polarization reduces substantially. These results are consistent with the previous study [5]. However, we found that the temperature dependent polarization is different from the previous study. In the present study, temperature dependent polarization keeps similar values till 195K ( $T/T_C \sim 0.56$ , where  $T_C$  is a Curie temperature.), while that reduces at a much low temperature in the previous study. We attribute the difference to the difference in the bulk sensitivity of the present study. The steep reduction of polarization at  $E_F$ , which is expected from the growth of NQP, was not observed clearly within the experimental accuracy.

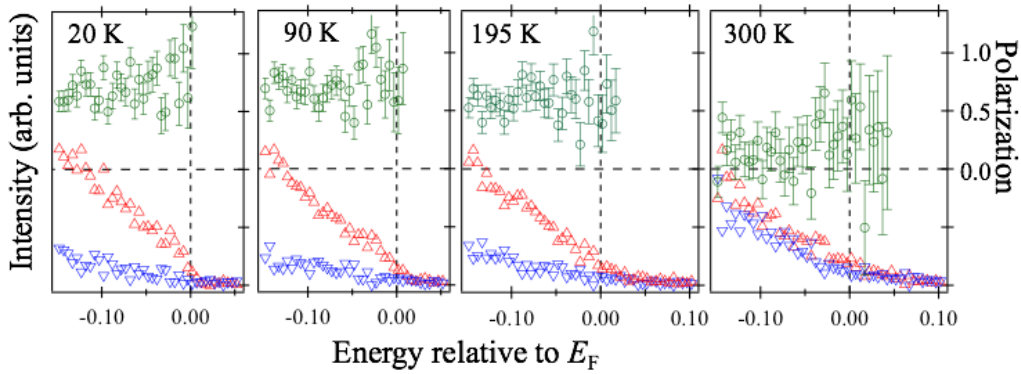


Fig. 1. Temperature dependent HRSRPES spectra and polarizations of  $\text{La}_{1-x}\text{Sr}_x\text{MnO}_3$ . The red triangles, blue triangles, and green circles show the majority spin spectrum, the minority spin spectrum, and polarization, respectively.

### ACKNOWLEDGEMENT

This work was partially supported by JSPS KAKENHI Grand Numbers (JP20H0185313) from MEXT.

### REFERENCES

- [1] M.I. Katsnelson *et al.*, *Rev. Mod. Phys.* **80**, 315-378 (2008).
- [2] V.Y. Irkhin and M.I. Katsnelson, *Usp. Fiz. Nauk* **164**, 705 (1994).
- [3] H. Fujiwara *et al.*, *Phys. Rev. Lett.* **121**, 257201 (2018).
- [4] K. Yaji *et al.*, *Rev. Sci. Instrum.* **87**, 053111 (2016).
- [5] J.-H. Park *et al.*, *Nature* **392**, 794-796 (1998).

# LIGHT POLARIZATION DEPENDENCE OF LOW-ENERGY ANGLE-RESOLVED PHOTOEMISSION SPECTROSCOPY OF A TRANSITION METAL DICHALCOGENIDE

Hiroaki Tanaka

*The Institute for Solid State Physics, The University of Tokyo*

Angle-resolved photoemission spectroscopy (ARPES) has been utilized to observe the band dispersion of crystals experimentally [1]. In ARPES measurements, X-ray or vacuum ultraviolet (VUV) light is irradiated on the crystal surface, and emitted photoelectrons are analyzed. The energy and momentum conservation laws determine the relationship between the Bloch wavevector and the binding energy, in other words, the band dispersion of solids.

As well as the band dispersion determined by ARPES, the photoemission intensity gives deeper insight into the electronic structure of solids because it is determined by the matrix element between the initial states (wave functions of the ground state) and the final states (approximated to plane waves). For example, the light polarization dependence of ARPES spectra has revealed orbital contributions of valence bands in the iron-based superconductor FeSe [2, 3]. Our study aims to quantitatively discuss the photoemission intensity distribution by combining the high-resolution ARPES and the photoemission intensity calculations based on the first-principles calculations.

We used the laser-based ARPES setup constructed at the Institute for Solid State Physics, the Univ. of Tokyo [4]. The photon energy was 7 eV, and the light polarization varied from  $\theta = 0^\circ$  (*s*-polarization) to  $\theta = 180^\circ$ , where  $\theta = 90^\circ$  is the *p*-polarization. The measurement temperature was around 60 K, and the energy resolution was 13 meV.

We measured the photoemission spectra of the transition metal dichalcogenide 1T-TiS<sub>2</sub> [Fig. 1(a)]. TiS<sub>2</sub> is a simple one-layered material, so we don't need to consider the termination surface dependence. No structure transition, such as the charge density wave phase, has been reported. Therefore, TiS<sub>2</sub> is suitable for quantitatively analyzing the photoemission intensity by experiments and numerical simulations. The band dispersion of 1T-TiS<sub>2</sub> has two hole bands near the  $\Gamma$  point [Fig. 1(b)]. Since these bands have only weak  $k_z$  dispersion, as described by slightly thick slab band dispersion, we can expect that they can be observed whatever photon energy is used.

Figures 1(c) and 1(d) summarize our ARPES measurements. When we used *s*-polarized light, the heavy hole band [blue curves in Fig. 1(c)] strongly contributed to the photoemission intensity. On the other hand, when *p*-polarized light was used, the light hole band [red curves in Fig. 1(d)] was dominant. This difference reflects the orbital selectivity of the photoemission process and its dependence on incident light polarization.

We investigated the light polarization dependence by changing the angle  $\theta$  with a  $10^\circ$  step. Since the  $\lambda/2$  waveplate installed in the laser-ARPES setup can be mechanically controlled, we could measure the polarization dependence automatically using a Python program. Figure 1(d) shows the result. As discussed above, the peak position in the *p*-polarized light measurements is about 50 meV lower than in the *s*-polarized case. More important is that the polarization dependence of the peak position exhibits a smooth curve. When we consider the bulk band dispersion comprising heavy and light hole bands, one of two peaks or both peaks should appear. However, we observed that the spectrum peak could appear between two hole bands, even though the VUV-ARPES using 7 eV laser is considered relatively bulk sensitive due to the long inelastic mean free path [5]. This result clearly shows that the surface electronic structure should be considered to discuss the polarization dependence of ARPES spectra.

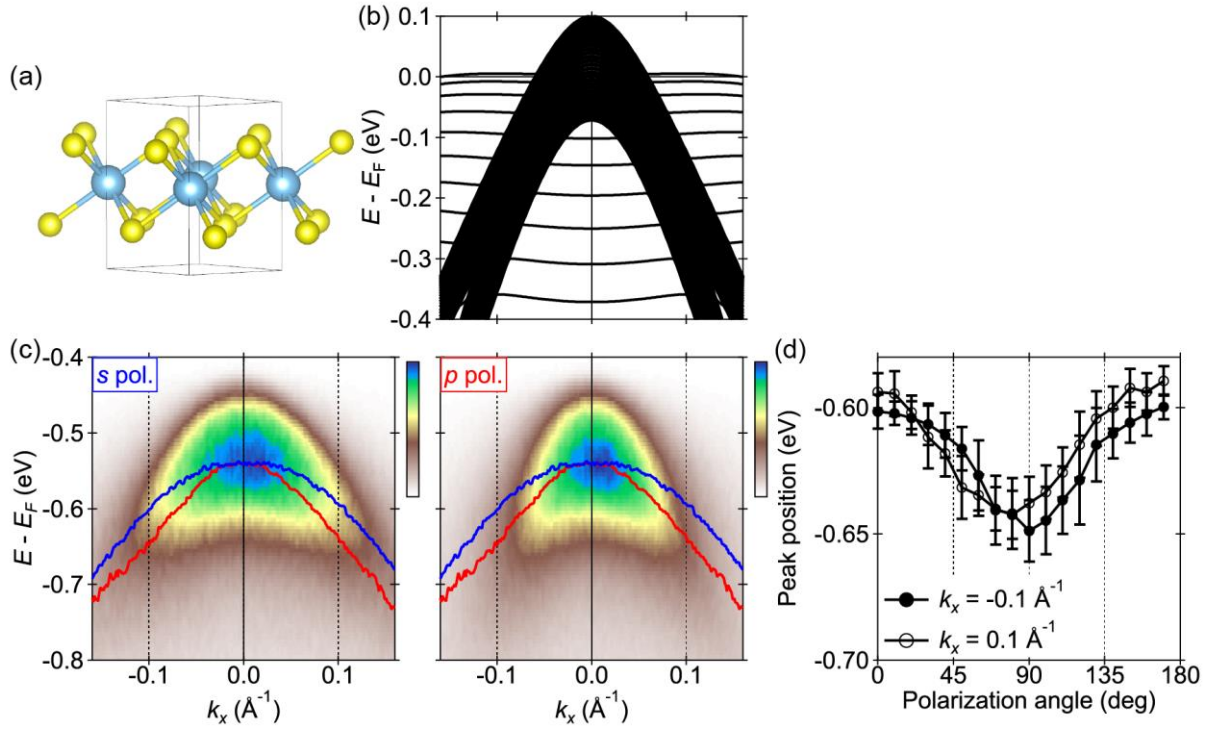


Figure 1: ARPES measurements of 1T-TiS<sub>2</sub>. (a) Crystal structure. (b) Calculated slab band dispersion along the  $\Gamma K$  ( $k_x$ ) direction. (c) Experimental band dispersion taken by  $s$ - and  $p$ -polarized light. The blue and red curves represent peak positions extracted from energy distribution curves in  $s$ - and  $p$ -polarization measurements. (d) Light polarization dependence of the peak position at  $k_x = -0.1 \text{ \AA}^{-1}$  and  $0.1 \text{ \AA}^{-1}$ .

In summary, we investigated the polarization dependence of ARPES spectra using the transition metal dichalcogenide 1T-TiS<sub>2</sub> and a high-resolution VUV-ARPES machine equipped with a 7 eV laser. We observed that the peak position of the hole bands oscillated by changing the light polarization. Such a continuous change cannot be explained by the bulk band dispersion of 1T-TiS<sub>2</sub>, so we will need to employ a slab system and detailed photoemission intensity calculations to reproduce the results theoretically.

## REFERENCES

- [1] J. A. Sobota *et al.*, Rev. Mod. Phys. **93**, 025006 (2021).
- [2] M. Ti *et al.*, Phys. Rev. X **9**, 041049 (2019).
- [3] R. P. Day *et al.*, npj Quantum Materials **4**, 54 (2019).
- [4] K. Yaji *et al.*, Rev. Sci. Instrum. **87**, 053111 (2016).
- [5] M. P. Seah and W. A. Dench, Surf. Interf. Anal. **1**, 2 (1979).

# SURFACE STATE SPIN POLARIZATION MEASUREMENT OF Co DOPED LaFeAsO

Soonsang Huh<sup>1</sup>, Yuto Fukushima<sup>1</sup>, Kaishu Kawaguchi<sup>1</sup>, Ayumi Harasawa<sup>1</sup>, Felix Anger<sup>2</sup>,  
Wurmehl Sabine<sup>2</sup>, Bernd Büchner<sup>2,3</sup>, and Takeshi Kondo<sup>1</sup>

1. *The Institute for Solid State Physics (ISSP), The University of Tokyo, Kashiwa, Chiba 277-8581, Japan*  
2. *Leibniz Institute for Solid State and Materials Research, IFW-Dresden, 01069, Dresden, Germany*  
3. *Institute of Solid State Physics, TU Dresden, 01069, Dresden, Germany*

The discovery of the superconductivity in F-doped LaFeAsO has opened new era for iron-based superconductors and brought renew interest in high  $T_C$  superconductivity research [1]. Extensive and intensive studies have shown that the Oxypnictide system, so called 1111 crystal structure system, exhibits relatively high  $T_C$  than other systems. Up to now, SmFeAsO<sub>1-x</sub> ( $T_C \sim 55$  K) has been observed with the highest  $T_C$  in bulk single crystal at ambient pressure among iron-based superconductors [2]. For this reason, understanding the mechanism that why high  $T_C$  favor in this crystal structure become one of the main issues in the research field.

In this regard, several angle-resolved photoemission spectroscopy (ARPES) experiments were conducted to understand the electronic structure, which is believed to provide important clues to the high  $T_C$  mechanism. However, the 1111 system shows a polarized cleaved surface arising from both Lanthanide Oxides layer and Iron Pnictogen layer, resulting in a complex electronic structure. For example, [LaO]<sup>+</sup> layer and [FeAs]<sup>-</sup> layer exists in LaFeAsO. This leads to coexistence of surface and bulk electronic state. Although there are several studies reporting surface and bulk state [3, 4], still it is not clearly defined.

In this study, ARPES measurement were performed on 6% Co-doped LaFeAsO single crystal which is synthesized by solid state crystal growth technique [5]. Figures 1 (a) and (b) show Fermi surface taken at 10 K with photon energy of 40 eV and 7 eV, respectively. Fermi surface area of 7 eV data corresponds to red dashed box in Fig. 1 (a). Two large circular pockets are observed in both data. High symmetry cut along  $\Gamma - M$  direction is shown in Fig. 1 (c). Two electron band like dispersion is

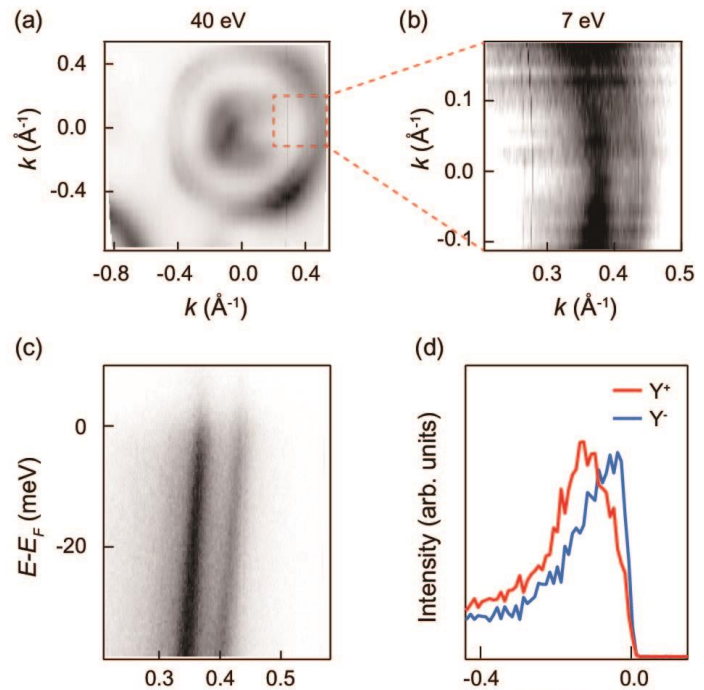


[Figure 1] Fermi surface taken by (a) 40 eV and (b) 7 eV. (c) High symmetry cut data taken along  $\Gamma - M$  direction. (d) Spin resolved energy distribution curve. Red and blue line indicates  $Y^+$  and  $Y^-$  spin direction measurement result, respectively.

observed around  $k = 0.4 \text{ \AA}^{-1}$ . According to previous calculations, the observed bands are expected to be the surface state. We tested the spin polarization of the this observed surface states. Surprisingly, opposite spin polarization is observed between the two bands. Spin polarization is likely due to the presence of inversion symmetry breaking in this surface state. However, the cause of this spin polarization needs to be elucidated through further experimental/theoretical studies.

## REFERENCES

- [1] Y. Kamihara, T. Watanabe, M. Hirano, and H. Hosono, *J. Am. Chem. Soc.* **130**, 3296 (2008).
- [2] Z.-A. Ren *et al.*, *Chin. Phys. Lett.* **25**, 2215 (2008)
- [3] L. X. Yang *et al.*, *Phys. Rev. B* **82**, 104519 (2010).
- [4] P. Zhang *et al.*, *Phys. Rev. B* **94**, 104517 (2016).
- [5] R. Kappenberger *et al.*, *J. Cryst. Growth* **483**, 9 (2018).

# THICKNESS DEPENDENCE OF SPIN-POLARIZED BAND STRUCTURE IN TOPOLOGICAL INSULATOR $\text{Bi}_2\text{Te}_3$ THIN FILMS

Kaishu Kawaguchi<sup>1</sup>, Ryo Mori<sup>1</sup>, Yuto Fukushima<sup>1</sup>, Hiroaki Tanaka<sup>1</sup>, Shinichiro Hatta<sup>2</sup>,  
Ayumi Harasawa<sup>1</sup>, Tetsuya Aruga<sup>2</sup>, Takeshi Kondo<sup>1</sup>

<sup>1</sup>ISSP, The University of Tokyo

<sup>2</sup>Graduate School of Science, Kyoto University

## INTRODUCTION

Topological insulators, with their surface state exhibiting spin-polarized electronic states on the surface, hold promising applications in spintronics and quantum information, and so on. In this context, employing thin films to enhance surface effects is a key approach. Under this situation, interference effects occur between the electronic states present at the surface and interface [1]. And additionally, energy splits in band dispersion also occur originating from the substrate effects [1,2]. In particular, substrate effects, when viewed from a macroscopic perspective, can be considered as a kind of the Rashba effect resulting from broken inversion asymmetry from the interface between thin films and substrate, called structure inversion asymmetry (SIA) [2]. This offers exciting prospects of merging different physical properties through junctions with superconductors [3] and so on. However, these SIA largely depend on the substrate type and controlling them can be challenging due to the varying origins and quantitative differences of potential modulation. Therefore, it is crucial to reveal the more microscopic origins of SIA, details about the potential structure and its origins that were previously unclear. For this purpose, we have extensively investigated the thickness and substrate dependency of the energy splitting structure in the thin films of the topological insulator  $\text{Bi}_2\text{Te}_3$ , to explore how potential modulation can be controlled.

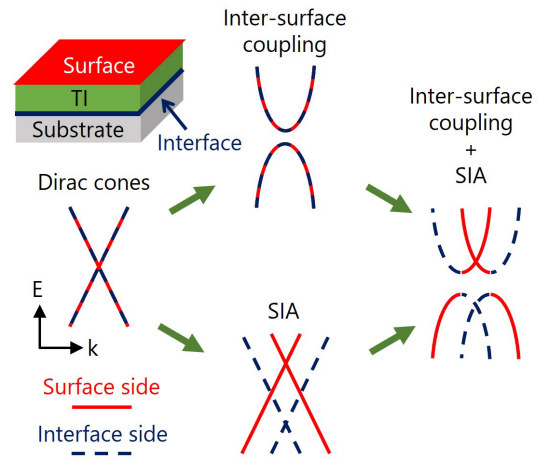


Fig. 1 : Band-dispersive depiction of energy-splitting structures originating from the hybridization of topological surface and interface states and SIA in topological insulator thin films.

## METHODS

A challenge in this research lies in the fact that each energy-split band dispersion is localized at the surface and interface. Therefore, it is difficult to identify the interface side in Angle-Resolved Photoemission Spectroscopy (ARPES) due to the decay of photoelectron intensity within the thin film. This complication, along with band broadening, can lead to obscured energy splitting, making observation impossible—a phenomenon reported in previous studies that calls for a solution. In this study, by using spin-resolved ARPES (SARPES) technics, we aimed to clearly separate the energy splitting structure based on the difference in spin polarization direction derived from the reversed helicity of the surface and interface.

For this study, considering the importance of insulating films in applications, experiments were conducted using a  $\text{CaF}_2/\text{Si}(111)$  substrate prepared by depositing a  $\text{CaF}_2$  thin film on a  $p$ -type  $\text{Si}(111)$  substrate.  $\text{Bi}_2\text{Te}_3$  ultra-thin films were prepared in ultra-high vacuum using a  $\text{Bi}_2\text{Te}_3$  deposition source [4]. The SARPES apparatus combines a Very Low Energy Electron Diffraction (VLEED) spin detector and a 7-eV laser to form a high-efficiency, high-resolution system [5] capable of decomposing even fine spin-split structures for efficient observation.

## RESULTS AND DISCUSSION

Figure 2 shows the thickness dependency of the  $\text{Bi}_2\text{Te}_3$  thin film made on the  $\text{CaF}_2/\text{Si}(111)$  substrate. A clear band structure can be observed, indicating high-quality thin film. Also, it is evident that a gap is formed at the Dirac point for less than 4 QL, aligning with previous research. Although the ARPES image does not reveal any energy-split behaviour, successful observation of the splitting structure was achieved by conducting spin-resolved measurements (Fig. 3). Furthermore, upon investigating the thickness dependency, an energy inversion of the spin-splitting structure was observed from 1 to 3 QL. Such an inversion phenomenon has never been observed in previous studies, making our research a first in this regard. Also, as the film thickness increases, a shift of the band to higher energy was noticed.

As possible origins of the energy split at the surface and interface, crystal structure distortion and peculiar charge transfer are considered. About structure distortion, it is especially noticeable when the film is thin [6]. On the other hand, if the charge is polarized towards the  $\text{Bi}_2\text{Te}_3$  side, the effect becomes significant when the film is thick. Therefore, it is believed that this inversion phenomenon of spin-splitting depending on the thickness arose due to the competition between these two effects. To understand these origins in more detail, it will be necessary to examine the doping dependence and to verify it through calculations.

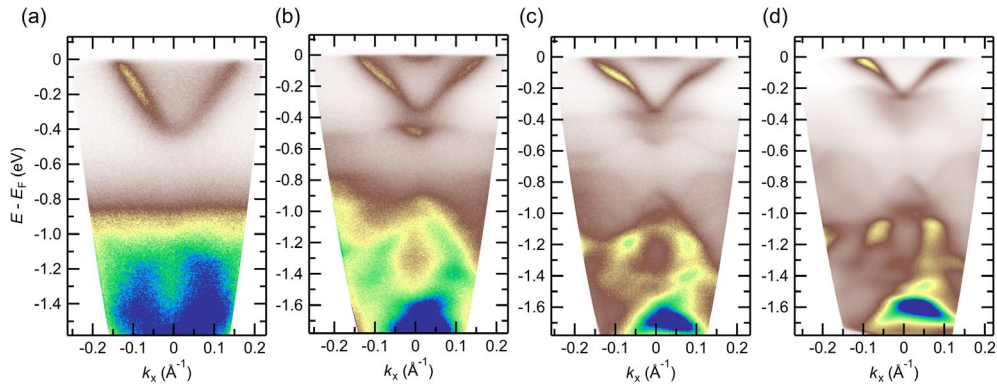


Fig. 2 : ARPES results of the thickness dependence of  $\text{Bi}_2\text{Te}_3$  thin films, for thicknesses of (a) 1 QL, (b) 2 QL, (c) 3 QL, and (d) 8 QL.

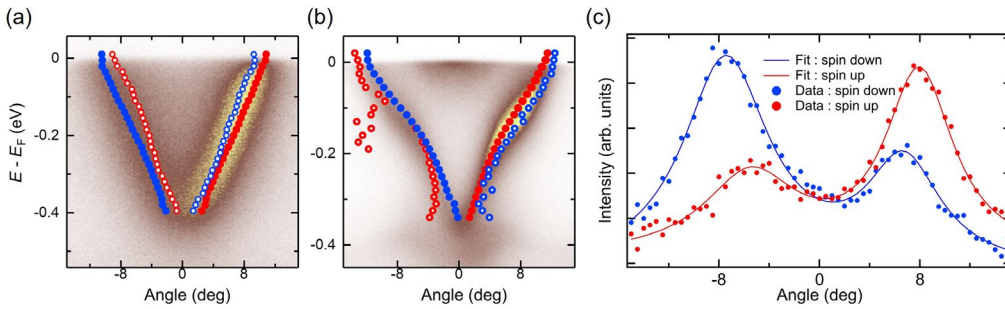


Fig. 3 : (a) 1 QL and (b) 3 QL, the peak positions obtained by fitting each spin-resolved ADC (angular distribution curve) spectrum are plotted on the ARPES image. The filling points indicate the spin up (red) and down (blue) peak positions for higher intensities and opaque points for lower intensities. (c) is ADC fitting result of (a) at  $E - E_F = -0.15$  eV.

## REFERENCES

- [1] H. Zhang *et al.*, Nat. Phys. **5**, 438 (2009).
- [2] Y. Zhang *et al.*, Nat. Phys. **6**, 584–588 (2010).
- [3] H. Yi *et al.*, Nat. Mater. **21**, 1366–1372 (2022).
- [4] S. Hatta *et al.*, Sci. Rep. **11**, 5742 (2021).
- [5] K. Yaji *et al.*, Rev. Sci. Instrum. **87**, 053111 (2016).
- [6] G. Landolt *et al.*, Phys. Rev. Lett. **112**, 057601 (2014).



# QUANTUM CONFINED SURFACE STATES FORMED IN A HEXAGONAL CORRAL IN SELF-ASSEMBLED HYDROGEN-BONDED ORGANIC FRAMEWORKS

Kaname Kanai<sup>1</sup>, Rena Moue<sup>1</sup>, Hiroto Yamazaki<sup>1</sup>, Kozo Mukai<sup>2</sup>, Kaishu Kawaguchi<sup>2</sup>, Yuto Fukushima<sup>2</sup>, Fumihiko Ozaki<sup>2</sup>, Ryo Mori<sup>2</sup>, Takeshi Kondo<sup>2</sup>, Ayumi Harasawa<sup>2</sup>, Shik Shin<sup>2</sup>, Jun Yoshinobu<sup>2</sup>

*Faculty of Science and Technology Tokyo University of Science<sup>1</sup>, The Institute for Solid State Physics, The University of Tokyo<sup>2</sup>*

The ability to control and modify the electronic properties of material surfaces is essential for the realization of next-generation devices involving electron and spin transfer at the interface between material surfaces and electrodes. In the field of surface science, the properties of many surface states and techniques for the modification of these surface states have been pursued. In particular, the Shockley state (SS), which is a pseudo-two-dimensional free electronic surface state on the (111) surface of an fcc-metal, is sensitive to various molecular adsorptions and has been the subject of many studies. However, SS is easily and quickly dissipated by irregularly adsorbed molecules. Meanwhile, for regularly arranged molecules on the surface, SS survives, and in some cases, its properties are significantly modified<sup>[1]</sup>. This indicates that the sensitivity of SS to adsorbates originates from a situation in which spatially spread pseudo-free electrons in two dimensions are easily scattered by the periodic potentials newly created parallel to the surface by the adsorbed molecular array. In such a situation, electron waves scattered by adsorbates regularly arranged to form void spaces, referred to as corrals, are expected to create standing waves inside the corrals.

In recent years, several studies have mentioned that molecules with a macrocyclic structure, superstructures made by adsorbing molecules on their surfaces and metal clusters, can create standing waves of electrons and have demonstrated quantum confinement in these structures. However, the formation of such quantum confined surface states (QCSSs) associated with molecular adsorption is mostly caused by accidentally self-assembled superstructures, and neither the corral size nor its shape is easily tunable. In this study, we propose another approach that is relatively robust to self-assembly imperfections, namely quantum confinement based on hydrogen-bonded organic frameworks (HOFs).

Carbon nitride molecule, melem (2,5,8-triamino-tri-s-triazine) has three-fold symmetry. Melem forms HOFs with characteristic structures by forming multiple hydrogen bonds between adjacent molecules in the crystal or on the surface. In general, many carbon nitride compounds that use hydrogen bonding as one of their cohesive forces have large voids in their crystal structures, which is also true for HOFs formed on the surface (SHOF). The SHOF is expected to form a graphite-like structure with a long-range order rather than a localized structure. Under these conditions, the SHOFs formed on the fcc-metal (111) surface are expected to produce identical confinement potentials in the corral created in their structures, resulting in the formation of a two-dimensional network of nearly identical QCSSs.

In this study, SHOFs were formed on Au(111) by melem, and their electronic structures were investigated by angle-resolved photoemission spectroscopy (ARPES). The presence of slightly distorted hexagonal corrals in the SHOF of melem with a honeycomb (HC) structure is expected to lead to quantum confinement of SSs of Au(111). Meanwhile, the confinement potential is created as a result of the slight displacement of the Au(111) surface atoms in the surface vertical direction, and the magnitude of the potential formed is small.

The SS of clean Au(111) observed by ARPES (Figure 1a) shows parabolic band dispersion as a quasi-two-dimensional free-electron system. The SS band exhibits a large Rashba splitting characteristic of Au(111). This large splitting is because the SS of Au(111) has a strongly asymmetric wave function near the outermost nuclei of the Au atoms. The effective

mass of the SS electron was estimated to be  $m^* = (0.274 \pm 0.020) m_e$ . the coverages of the melem layers at 1 and 2 Å correspond to the coverages of the submonolayers, and the melem layer has a HC structure. The band mapping results of Melem(1 Å)/Au(111) (Figure 1b) clearly show that the SS band shape of Au(111) is different from that of pristine Au(111). ARPES band mapping showed no Rashba splitting and a single broad weak energy band. In contrast, a localized state with a narrow dispersion width, which does not exist in pristine Au(111), is newly formed at approximately 0.40 and 0.47 eV. Since the highest occupied molecular orbital of the melem appears below a binding energy of 2 eV, these localized states are not derived from the melem itself.

To examine the detailed band dispersion of this localized state, curve fitting was performed for each energy distribution curve, and the results are shown by black dashed lines in Figure 1b. This result also shows that the dispersion width is extremely narrow compared with that of the SS. In contrast, this level was slightly curved, indicating slight dispersion. The band mapping results of Melem(2 Å)/Au(111) by ARPES intensity (Figure 1c) were very similar to those of Melem(1 Å)/Au(111), with a localized state observed near the bottom of the SS. In contrast, the fitting analysis shows that the dispersion widths of the two localized states are slightly smaller than those of Melem(1 Å)/Au(111), indicating a more localized nature. The discrete states present in Melem(1 Å)/Au(111) and Melem(2 Å)/Au(111) suddenly disappeared in both the ARPES (Figure 1d) of Melem(3 Å)/Au(111). From the results of LEED experiments, when the coverage of the melem layer reached 3 Å, a monolayer was formed in which the closed-packed structure was dominant. This abrupt change in the surface electronic structure strongly suggests that the localized states originates from the HC structure and that this is the QCSSs in the corral of the HC structure. Melem(3 Å)/Au(111), where the closed-packed structure is dominant, does not have a corral similar to the HC structure, which can be interpreted as the disappearance of the localized states observed in the HC structure because quantum confinement of the surface electrons does not occur.

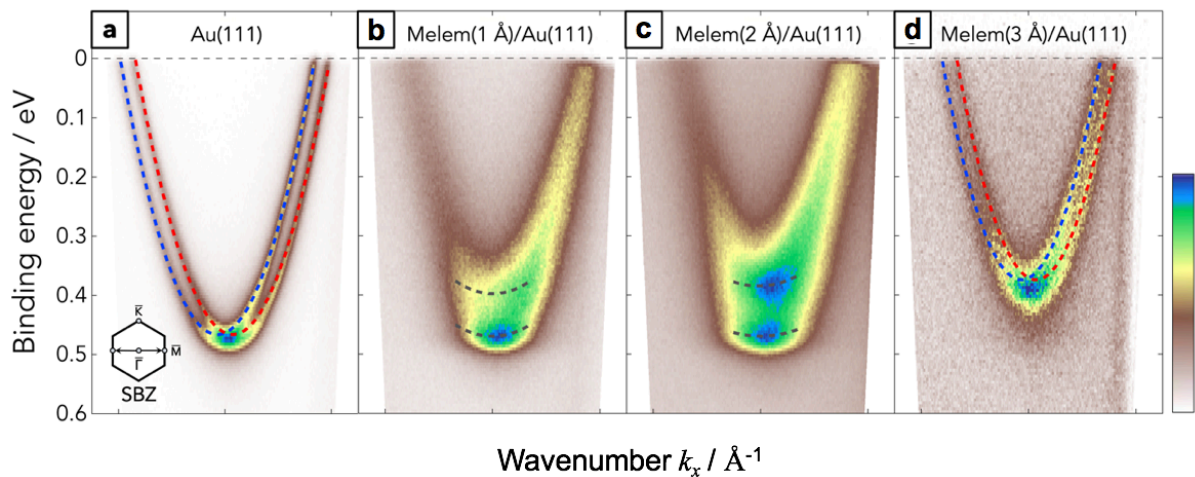


Figure 1. Band mapping around the  $\Gamma$  point ( $k_x = 0 \text{ \AA}^{-1}$ ) of a) clean Au(111), b) melem(1 Å)/Au(111), c) melem(2 Å)/Au(111), and d) melem(3 Å)/Au(111) by angle-resolved photoemission spectroscopy (ARPES).

## REFERENCE

- [1] R. Moue *et al.*, *Adv. Mater. Inter.*, **2022**, 2201102 (2022).

# STUDY ON SPIN STRUCTURE OF THE SURFACE STATE IN TYPE-II WEYL SEMIMETAL NbIrTe<sub>4</sub>

Soonsang Huh<sup>1</sup>, Soohyun Cho<sup>2</sup>, Wei Xia<sup>3,4</sup>, Soonsang Huh<sup>1</sup>, Yuto Fukushima<sup>1</sup>, Ayumi Harasawa<sup>1</sup>, Takeshi Kondo<sup>1,5</sup>, Yanfeng Guo<sup>3,4</sup> and Dawei Shen<sup>2\*</sup>

1. *Institute for Solid State Physics, University of Tokyo, Kashiwa 277-8581, Japan*
2. *National Synchrotron Radiation Laboratory, University of Science and Technology of China, Hefei 230029, China*
3. *School of Physical Science and Technology, Shanghai Tech University, 201210, Shanghai, China*
4. *Shanghai Tech Laboratory for Topological Physics, Shanghai Tech University, 201210, Shanghai, China*
5. *Trans-scale Quantum Science Institute, University of Tokyo, Tokyo 113-0033, Japan.*

The topological Weyl semimetals (TWS) originate from their unusual bulk electronic structure and have the nondegenerate bands crossing in a single point of  $\mathbf{k}$  space, so-called the Weyl point. This can be realized in the quantum materials where either time-reversal or inversion symmetry, or both, is broken [1-3]. The symmetry tends to produce copies of Weyl points and separate the Weyl nodes with different non-zero Chern number in the Brillouin zone. On the boundary, topological edge states exist at edges of 2D planes and disappear at edges of other planes in which the separation points between two types of planes are Weyl points [1]. Therefore, the Fermi surface of the TWS simply consist of only two such points and show an opened line that connect each pair of Weyl nodes with opposite chirality, which is called a Fermi arc [1-3]. Moreover, in  $\text{Mo}_x\text{W}_{1-x}\text{Te}_2$  compound, another type of the TWS has been discovered with called type-II TWS whose Weyl nodes are highly anisotropic and tilted, breaking the Lorentz symmetry [1-5]. Given the feature of the band touching at the Weyl node, the Fermi surface at the Weyl nodes of the type-II WSM exhibit the electron and hole pockets [2-5]. This distinction feature of the band touching near the Weyl node may give a rise to marked differences in the thermodynamics and response to external magnetic field [2-5].

Recently, it has been reported that  $(\text{Nb}, \text{Ta})\text{IrTe}_4$  is a ternary TWS of type-II [3-5]. This compound crystallizes in a non-centrosymmetric orthorhombic lattice with space group  $\text{Pmn}2_1$  (No. 31) and have van der Waals interaction within layers [3-5]. Figure 1a show the side and top view of the crystal structure in  $\text{NbIrTe}_4$ , which show that the Nb and Ir atoms are octahedrally coordinated by Te atoms. The structural symmetry and a stacking configuration of  $\text{NbIrTe}_4$  is identical structure with the orthorhombic  $1\text{T}_d\text{-MX}_2$  ( $\text{M} = \text{Mo}, \text{W}$ ;  $\text{X} = \text{S}, \text{Se}, \text{Te}$ ) as the first suggestion with the type-II WSM, but  $\text{NbIrTe}_4$  has a unit cell doubled along  $\mathbf{b}$  direction and the substitution from M atoms in  $1\text{T}_d\text{-MX}_2$  to Nb and Ir atoms in  $\text{NbIrTe}_4$  [3-5]. Because of the similarity in the crystal structure,  $\text{NbIrTe}_4$  has the Nb-Ir chain as shown in the top view of Fig. 1a, which is similar with the Mo-Mo or W-W chain that can be related to the unusual electronic transport in  $1\text{T}_d\text{-MX}_2$ . The Nb-Ir chain is along the  $\mathbf{a}$  and  $\Gamma$  to X direction in the crystal and Brillouin zone (BZ) coordinates in Figs. 1a and 1b, respectively. Figure 1b

shows the orthorhombic bulk BZ and projected surface BZ onto the (001) surface with the high symmetry points.

In this study, we investigate the electronic and spin structure of the surface state in NbIrTe<sub>4</sub> utilizing high-resolution angle- and spin- resolved photoemission spectroscopy. The low-energy photoemission spectra taken from the laser-based ARPES with 6.994 eV photons clearly describe the fine dispersion of the surface state near the Y point with the higher momentum resolution in Figs. 1 (c) and (d). In previous ARPES study in Refs. [5], NbIrTe<sub>4</sub> show the Weyl points between the  $\Gamma$  and Y points, and the Weyl nodes would be connected by the surface state along  $k_y$  direction in Fig. 1(c). In our band calculation, the surface state at Y point show the spin-polarization along the  $+s_y$  or  $-s_y$  direction, but we cannot obtain the opposite sign of the spin-resolved energy distribution curves (EDCs) between  $-k_F$  and  $+k_F$  as shown in Figs. 1(e) and (f). For the experiment failure to show the spin texture in the surface state, we speculate that there could be a possibility to be a photoelectron interference effects in the surface state [6].

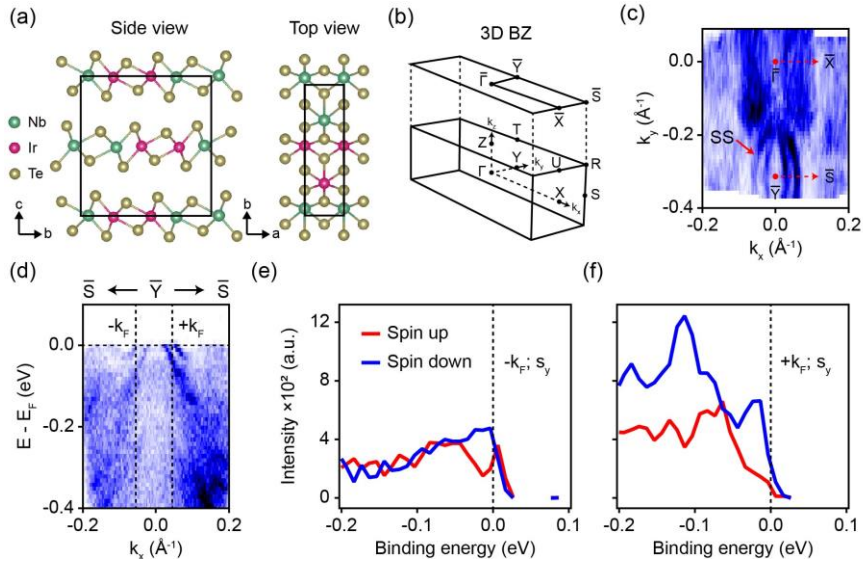


Figure 1. (a) The top and side view of the crystal structure of NbIrTe<sub>4</sub>. (b) The orthorhombic bulk BZ and projected surface BZ onto the (001) surface with the high symmetry points. (c) Experimentally obtained Fermi surface at 6.994 eV and 15 K. (d) The ARPES spectra along the S-Y-S direction. The spin-resolved EDCs of the surface state at  $-k_F$  (e) and  $+k_F$  (f) as marked in d. The spin-resolved EDCs represent spin texture along the  $s_y$  direction.

## REFERENCES

- [1] C. Zhang *et al.*, Annu. Rev. Mater. Res. **2020**, 50:131-153.
- [2] A. A. Soluyanov *et al.*, Nature **2015**, 527 495.
- [3] Ilya Belopolski *et al.*, Nat. Commun. **2017**, 8 942.
- [4] E. Haubold *et al.*, Phys. Rev. B **2017**, 95 241108(R).
- [5] S. A. Ekehana *et al.*, Phys. Rev. B **2020**, 102 085126.
- [6] Z.-H. Zhu *et al.*, Phys. Rev. Lett. **2014**, 112 076802.